Three-dimensional skyrmion states in thin films of cubic helimagnets

F. N. Rybakov,[1,2,*] A. B. Borisov,[1] and A. N. Bogdanov[2,†]
[1]*Institute of Metal Physics, Ekaterinburg 620990, Russia*
[2]*IFW Dresden, Postfach 270116, D-01171 Dresden, Germany*
(Received 20 September 2012; revised manuscript received 2 March 2013; published 28 March 2013)

A direct three-dimensional minimization of the standard energy functional shows that in thin films of cubic helimagnets, chiral skyrmions are modulated along three spatial directions. The structure of such three-dimensional skyrmions can be thought of as a superposition of conical modulations along the skyrmion axis and double-twist rotation in the perpendicular plane. We show that chiral modulations across the layer thickness radically change the skyrmion energetics and provide a thermodynamical stability of a skyrmion lattice in a broad range of applied magnetic fields. These results disclose a basic physical mechanism underlying the formation of skyrmion states recently observed in nanolayers of cubic helimagnets.

DOI: 10.1103/PhysRevB.87.094424 PACS number(s): 75.10.−b, 75.30.Kz, 75.70.−i

The concept of multidimensional topological solitons (*skyrmions*) plays an important role in describing a wide-range of physical phenomena in many physical systems, including hadrons and nuclear matter, condensed-matter systems, cosmology, and astrophysics.[1–3] In the majority of nonlinear field models, skyrmions are unstable and collapse spontaneously into topological singularities.[4] It was proven mathematically, however, that in noncentrosymmetric nonlinear systems, magnetic interactions imposed by the handedness of the underlaying structure provide a specific stabilization mechanism for two- and three-dimensional (2D and 3D) solitons (so called *chiral* skyrmions).[5] This singles out nonlinear models with broken chiral symmetry as a special class of systems, where chiral skyrmions can be formed as static, *mesoscopic* 2D and 3D solitons in broad ranges of the thermodynamical parameters.[5–7]

Recent direct observations of chiral skyrmions in thin layers of (Fe,Co)Si cubic helimagnets[8] have triggered an intensive search and investigations of similar skyrmionic states in chiral condensed-matter systems, including noncentrosymmetric magnets,[9,10] multiferroics,[11] liquid crystals,[12] and nanolayers of magnetic metals with induced chiral interactions.[13]

The experimental observations of skyrmion states in thin layers of cubic helimagnets[8–11] are in obvious contrast to the magnetic properties of bulk cubic helimagnets where one-dimensional (*conical*) modulations correspond to the global minimum of the system, and skyrmions can exist only as metastable states.[6,14] Generally, the exact magnetic structures of modulated states arising in confined cubic helimagnets are still not resolved, and the physical mechanisms underlying their stability are an open question.

In this paper, we provide three-dimensional calculations of chiral modulated states in thin layers of cubic helimagnet films. We show that below a critical thickness, a double-twist skyrmion gains additional modulations along its axis. The calculated phase diagram for 3D skyrmions and competing phases indicates a broad range of film thickness, where skyrmionic states are thermodynamically stable.

Within the phenomenological theory introduced by Dzyaloshinskii,[15] the magnetic energy density of a cubic noncentrosymmetric ferromagnet can be written as[15,16]

$$w = A\,(\mathbf{grad}\,\mathbf{m})^2 + D\,\mathbf{m}\cdot\mathrm{rot}\,\mathbf{m} - \mathbf{H}\cdot\mathbf{m}\,M, \qquad (1)$$

where $\mathbf{m} = (\sin\theta\cos\psi; \sin\theta\sin\psi; \cos\theta)$ is the unity vector along the magnetization $\mathbf{M}$ and $\mathbf{H}$ is the applied field. Energy density functional (1) includes only the principal interactions essential to stabilize skyrmions and helicoids: the exchange stiffness with constant A, Dzyaloshinskii-Moriya (DM) coupling energy with constant D, and the Zeeman energy. We neglect less important energy contributions such as intrinsic and induced magnetic anisotropies or stray fields. In contrast to common magnetic bubbles arising due to surface magnetodipole forces,[17] chiral skyrmions are stabilized by internal short-range interactions.[6,18] Generally stray-field effects in noncentrosymmetric magnets are found to be weak due to the stabilizing influence of the DM interactions.[18]

DM interactions favor spatial modulations of $\mathbf{M}$ with a fixed rotation sense.[15] In an infinite sample, isolated skyrmions [Fig. 1(a)] are described by solutions of the type[5,6]

$$\theta = \theta(\rho), \quad \psi = \varphi + \pi/2. \qquad (2)$$

Here we write the spatial variables in terms of cylindrical coordinates $\boldsymbol{r} = (\rho\cos\varphi; \rho\sin\varphi; z)$. Equation (2) describes 2D skyrmions as axisymmetric tubes with "double-twist" modulations in the (x, y) plane and a homogeneous distribution along the skyrmion axis (z axis) [Fig. 1(a)].[6,19] The solutions for one-dimensional modulations include distorted helices with the propagation direction perpendicular to the applied field, *helicoids* [Fig. 1(b)], and longitudinal distorted helices modulated along the field, *cones* [Fig. 1(d)]. The analytical solutions for helicoids describe a gradual unwinding of chiral coils in an increasing magnetic field.[15] The equilibrium parameters for the cone phase are given by[16]

$$\cos\theta = |\mathbf{H}|/H_D, \quad \psi(z) = \psi_{\mathrm{cone}}(z) \equiv 2\pi z/L_D, \qquad (3)$$

where the period of the helix, L_D, and the saturation field, H_D, are expressed as

$$L_D = 4\pi A/|D|, \quad H_D = D^2/(2AM). \qquad (4)$$

We introduce the reduced energy density of a modulate phase as $e = \langle w\rangle/[D^2/(4A)]$, where $\langle w\rangle$ is the energy density averaged over the modulation period. Then the equilibrium energy density of the cone phase can be written as

$$e_{\mathrm{cone}} = -[1 + (H/H_D)^2]. \qquad (5)$$

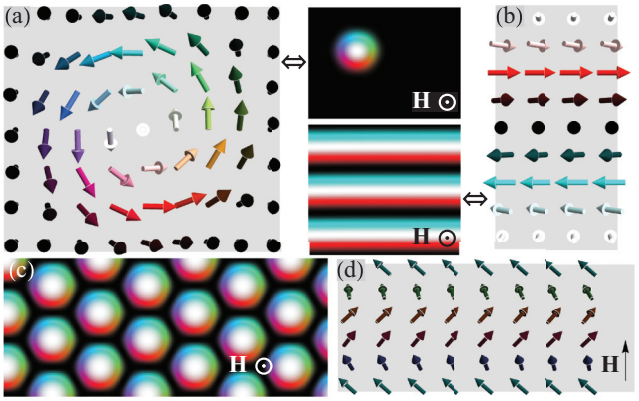

FIG. 1. (Color online) Magnetic configurations in basic chiral modulations arising in cubic helimagnets: (a) an isolated skyrmion with double-twist modulations perpendicular to the applied field, (b) transversally distorted helices (*helicoids*), (c) a hexagonal lattices of chiral skyrmions (a), and (d) longitudinal distorted helices (*cones*).

In an infinite sample, the cone (3) corresponds to the global minimum of model (1) in the entire magnetic field range below the saturation field H_D (4). Helicoids and skyrmion lattices only exist as metastable states.[14]

Contrary to lower symmetry noncentrosymmetric ferromagnets,[5] in cubic helimagnets DM interactions provide *three* equivalent modulation directions. However, 2D chiral skyrmions investigated in Refs. 6 and 20 have only two (in-plane) modulation directions while along the skyrmion axis the structure remains homogeneous. Thus, the following question arises: *is it possible to lower the skyrmion energy by imposing additional chiral modulations along the skyrmion axis?* Our calculations based on rigorous solutions of micromagnetic equations show that the formation of 3D skyrmions actually occurs in the thickness range below a critical thickness.

As a model, we consider a film of thickness L, infinite in the x and y directions and bounded by parallel planes at $z = \pm L/2$. Numerical solutions for chiral modulations are derived by direct minimization of functional (1) with free boundary conditions along the z axis and periodic boundary conditions in the (x,y) plane. This yields the equilibrium spatially inhomogeneous distributions of the magnetization vector $\mathbf{m}$ in the layer as functions of the three spatial variables and the two control parameters, namely the reduced magnetic field H/H_D and the *confinement ratio* L/L_D.

A three-dimensional minimization of nonlinear σ models needs huge computing efforts and is usually executed on high-performance supercomputers.[21] Modern graphics cards offer a promising alternative. However, this method requires special hardware-oriented highly parallel algorithms.[22] We have developed a special algorithm for CUDA architecture for NVIDIA graphics cards. This architecture has been found to be efficient in solving complex micromagnetic problems.[23] We use a nonlinear conjugate-gradient method to minimize energy functional (1). The results of the minimization have been checked based on their compatibility with the Euler-Lagrange equations. The results of numerical minimization of model (1) are presented in Figs. 2, 3, and 4 and as video files.[24]

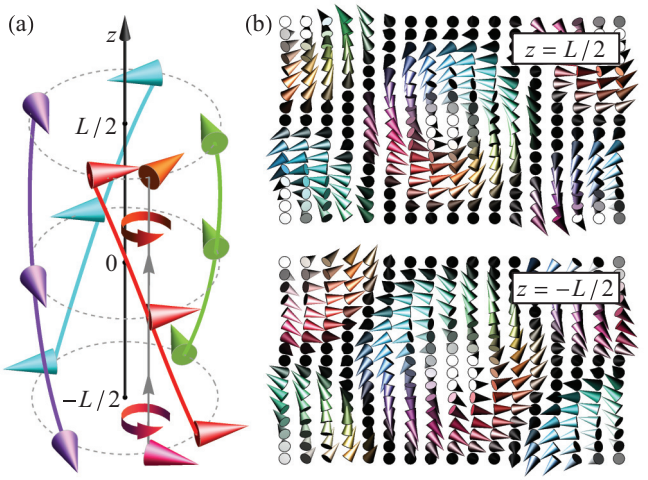

FIG. 2. (Color online) 3D skyrmion lattice: (a) Distribution of the magnetization in the skyrmion core demonstrates chiral conical modulations along the cell axis. For clarity, the sizes along the z axis are magnified; (b) calculated distribution of the magnetization in the skyrmion cell for top and bottom layers in a film with thickness $L/L_D = 0.25$ and in the applied field $H/H_D = 0.2$.

Isolated and embedded skyrmions. The equilibrium magnetic configurations in a 3D skyrmion lattice strongly differ from axisymmetric 2D skyrmions arising in infinite helimagnets (2). The magnetization vector $\mathbf{m}$ depends on all three spatial components, (ρ,φ,z), and exhibits complex three-dimensional modulations (Fig. 2 and Ref. 24). It was, however, found that a simplified ansatz

$$\theta = \theta(\rho), \quad \psi(\phi,z) = \varphi + \pi/2 + \widetilde{\psi}(z) \tag{6}$$

with $\widetilde{\psi}(z) = \psi_{\text{cone}}$ (3) provides a nice approximation of the solutions for isolated and bound 3D skyrmions.

Equation (6) describes double-twist rotations in the (x,y) plane and conical modulations (3) along the skyrmion axis [Fig. 2(a)]. Remarkably, the period of conical modulations in

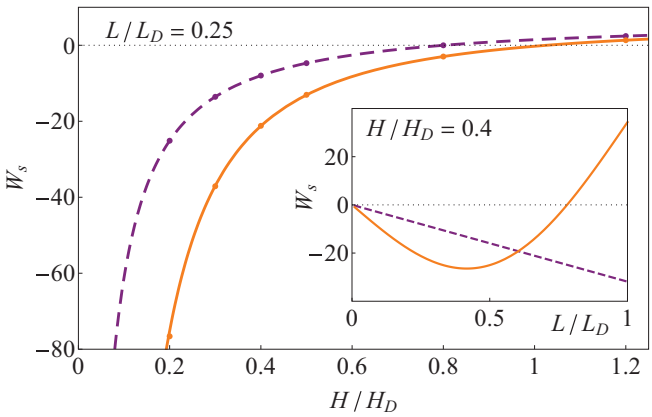

FIG. 3. (Color online) Calculated equilibrium energies of isolated skyrmions with ansatz (6) (solid line) and for those that are homogeneous along the z axis (2D skyrmions, dashed line) as functions of the reduced field H/H_D in a film with reduced thickness $L/L_D = 0.25$. The inset shows the equilibrium energies of the skyrmions as functions of the reduced thickness at a fixed applied field $H/H_D = 0.4$.

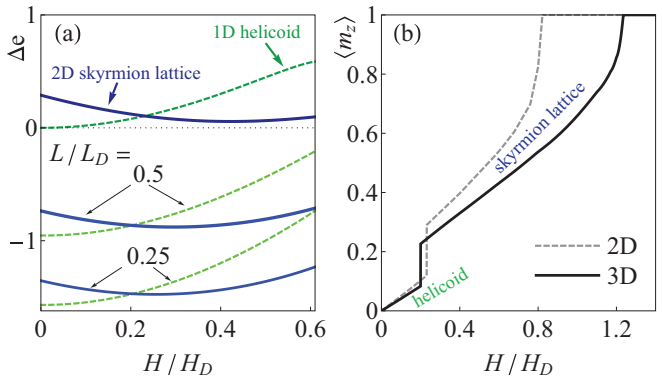

FIG. 4. (Color online) (a) The differences Δe between the energies of the skyrmion lattice and the cone phase (solid, blue) and between the helicoid and the cone phase (dashed, green) as functions of the applied field for 2D and 3D modulations. Functions $\Delta e(H/H_D)$ are plotted for two values of reduced film thicknesses $L/L_D = 0.25$ and 0.5 in comparison with results derived for 1D helicoids[15] and hexagonal skyrmion lattices homogeneous along the skyrmion axis (2D skyrmions investigated in Ref. 6). (b) Magnetization curves for 3D modulated structures in a film with reduced thickness $L/L_D = 0.25$ (solid lines) in comparison with the magnetization curves for 1D helicoids and 2D skyrmion lattices.[6,15]

the skyrmion coincides with the helix period, L_D. We introduce the reduced equilibrium energy of an isolated skyrmion as

$$W_s = \frac{1}{(A\,L_D)} \int_0^{2\pi} d\varphi \int_{-L/2}^{L/2} dz \int_0^{\infty} (w - w_0)\rho\, d\rho, \qquad (7)$$

where $w_0 = -HM$ is the energy density of the saturated state. In Fig. 3, the energies W_s for isolated skyrmions with ansatz (6) and for solutions homogeneous along the skyrmion axis (2D skyrmions) are plotted as functions of the applied field in Fig. 3 (main figure) and the reduced film thickness (inset). These results show that in a broad range of the control parameters H/H_D and L/L_D, the modulation along the skyrmion axis reduces its energy. 3D modulated skyrmions should not be confused with three-dimensional topological chiral solitons (*hopfions*).[7]

Helicoids and cones. In thin films, helicoids become inhomogeneous along the film thickness.[24] Conical states propagating perpendicular to the layer surfaces are compatible with the film geometry, and the free boundary conditions impose no constrictions on these modulations. As a result, the solutions for the cone phase in the film and the equilibrium energy density are equal to those in a bulk sample (3) and (5).[14,16] Conical states (3) can exist even in films with thickness smaller than the helix period ($L < L_D$) (4). In this case, $\Delta\psi = |\psi(L/2) - \psi(-L/2)| = 2\pi L/L_D < 2\pi$.

The calculated equilibrium energy densities of helicoids ($e_{\rm h}$) and 3D skyrmion lattices ($e_{\rm sk}$) have been compared with the cone energy density ($e_{\rm cone}$). The results are plotted as functions $\Delta e_{\rm h} = (e_{\rm h} - e_{\rm cone})$ and $\Delta e_{\rm sk} = (e_{\rm sk} - e_{\rm cone})$ versus the applied field together with the corresponding results for 1D helicoids and 2D skyrmion lattices arising in bulk cubic helimagnets[6,15] [Fig. 4(a)]. In the latter case, the cone has the lowest energy in the entire region below the saturation field, H_D (3). This situation retains in sufficiently thick films (see Fig. 3, inset). However, the energy balance between the chiral phases drastically changes in thin layers below the critical thickness. Here the formation of 3D modulations results in a large reduction of the helicoids and skyrmion lattices and leads to their energetic advantage over the cone phase [Fig. 4(a)]. This means that in sufficiently thin cubic helimagnet films, the onset of conical modulations in helicoids and skyrmion lattices provides a specific mechanism to stabilize these chiral modulations in a broad range of applied magnetic fields (Fig. 4).

An elementary analysis of modulations (6) allows us to understand basic physical mechanisms underlying the formation of 3D skyrmions. Inserting ansatz (6) into (1) yields the following expression:

$$\tilde{w} = A\left(\theta_\rho^2 + \frac{\sin^2\theta}{\rho^2}\right) + \underbrace{D\cos\widetilde{\psi}(z)}_{\widetilde{D}(z)}\left(\theta_\rho + \frac{\sin 2\theta}{2\rho}\right) - H\,M\cos\theta + \underbrace{\sin^2\theta\left[A\widetilde{\psi}_z^2(z) - D\widetilde{\psi}_z(z)\right]}_{w_z}. \qquad (8)$$

In functional (8), the first three terms are responsible for the formation of double-twist modulations in the (x,y) plane,[6] and $w_z(z)$ describes modulations along the skyrmion axis. With conical modes $\widetilde{\psi}(z) = \psi_{\rm cone}$ (3), the function $\widetilde{D}(z)$ and energy density w_z can be written as

$$\widetilde{D}(z) = D\cos(2\pi z/L_D), \quad w_z = -D^2\sin^2\theta/(4A). \qquad (9)$$

Energy density (8) includes two different DM terms. The first, with factor $\widetilde{D}(z)$, favors double-twist rotations in the (x,y) plane, the other induces cone-mode modulations along the z axis. The energy gain from the double-twist modulations $\propto\widetilde{D}^2(z)$ reaches the maximum at $\widetilde{\psi}(z) = 0$. The cone modulations increase the double-twist energy. On the other hand, these yield a negative energy contribution w_z (9) into the total energy. The equilibrium 3D skyrmion patterns are formed as a result of the competition between different DM interaction terms.

In the calculated 3D skyrmion textures, angle $\widetilde{\psi}$ equals zero in the layer center and rotates with a same rotation sense to the maximal value at the surfaces, $|\widetilde{\psi}(\pm L/2)| = \pi L/L_D$. Importantly, for $\widetilde{\psi} > \pi/2$ the factor $\widetilde{D}(z)$ becomes negative. This means that cubic helimagnet films with thickness larger than $L_D/2$ include regions where function $\widetilde{D}(z)$ becomes negative corresponding to the double-twist modes with an energetically unfavorable sense of rotation. This explains the existence of the critical thickness for 3D modulations and shows that its value is of the order of the helix period L_D (see, e.g., Fig. 3, inset).

The first direct observations of chiral skyrmions have been reported in a mechanically thinned cubic helimagnet (Fe,Co)Si with thickness $L = 20$ nm.[8] In this material, $L_D = 90$ nm, and thus the confinement ratio $L/L_D = 0.22$. This is quite below the critical thickness, and thus 3D modulations are expected to exist in this film. In Fig. 4(b), we present the calculated magnetization curve for a film with confinement ratio $L/L_D = 0.25$ close to that of the film investigated in Ref. 8. This indicates the stability regions for helicoids and skyrmions, the first-order transitions between helicoid and skyrmion lattices, and the second-order transition of the skyrmion lattice into the saturated state.

Earlier, an alternative mechanism to stabilize chiral skyrmions in cubic helimagnets was proposed in Ref. 14. According to these papers, the distortions of a cone phase imposed by uniaxial magnetic anisotropy strongly increase its energy. As a result, chiral skyrmion lattices and helicoids become thermodynamically stable in a broad range of applied magnetic fields. In our recent studies, the cone modes remained undistorted. The energetic advantage of 3D skyrmion lattices and helicoids is gained because 3D modulations grant a larger reduction of the DM energy than single-direction modulations in cone modes. New experiments are needed for detailed investigations of induced magnetic anisotropy and to resolve the exact magnetic structures in confined cubic helimagnets.

In conclusion, direct 3D minimization of energy functional (1) shows that in sufficiently thin cubic helimagnets films, the common one-dimensional modulations (conical helices) become unstable and are replaced by unconventional helicoids and skyrmion states modulated along the layer thickness [Fig. 4(a)]. Our results provide the first consistent theory of chiral modulations in confined cubic helimagnets and elucidate recent experiments in mechanically thinned nanolayers of MnSi and kindred compounds.[8,9,11]

We thank T. Monchesky for critically reading the manuscript and fruitful advice.

*Author to whom all correspondence should be addressed: f.n.rybakov@gmail.com
†a.bogdanov@ifw-dresden.de

[1] *The Multifaceted Skyrmion*, edited by G. E. Brown and M. Rho (World Scientific, New Jersey, 2010).
[2] G. E. Volovik, *The Universe in a Helium Droplet* (Clarendon, Oxford, 2003).
[3] U. K. Rößler, A. N. Bogdanov, and C. Pfleiderer, Nature (London) **442**, 797 (2006).
[4] G. H. Derrick, J. Math. Phys. **5**, 1252 (1964).
[5] A. N. Bogdanov and D. A. Yablonsky, Zh. Eksp. Teor. Fiz. **95**, 178 (1989) [Sov. Phys. JETP **68**, 101 (1989)]; A. Bogdanov, Pis'ma Zh. Eksp. Teor. Fiz. **62**, 231 (1995) [JETP Lett. **62**, 247 (1995)].
[6] A. Bogdanov and A. Hubert, J. Magn. Magn. Mater. **138**, 255 (1994); **195**, 182 (1999); A. N. Bogdanov, U. K. Rößler, and C. Pfleiderer, Physica B **359**, 1162 (2005).
[7] A. B. Borisov and F. N. Rybakov, Low Temp. Phys. **36**, 766 (2010).
[8] X. Z. Yu, Y. Onose, N. Kanazawa, J. H. Park, J. H. Han, Y. Matsui, N. Nagaosa, and Y. Tokura, Nature (London) **465**, 901 (2010).
[9] X. Z. Yu, N. Kanazawa, Y. Onose, K. Kimoto, W. Z. Zhang, S. Ishiwata, Y. Matsui, and Y. Tokura, Nat. Mater. **10**, 106 (2011); X. Z. Yu, N. Kanazawa, W. Z. Zhang, T. Nagai, T. Hara, K. Kimoto, Y. Matsui, Y. Onose, and Y. Tokura, Nat. Commun. **3**, 988 (2012); A. Tonomura, X. Yu, K. Yanagisawa, T. Matsuda, Y. Onose, N. Kanazawa, H. S. Park, and Y. Tokura, Nano Lett. **12**, 1673 (2012).
[10] S. X. Huang and C. L. Chien, Phys. Rev. Lett. **108**, 267201 (2012); M. N. Wilson, E. A. Karhu, A. S. Quigley, U. K. Rößler, A. B. Butenko, A. N. Bogdanov, M. D. Robertson, and T. L. Monchesky, Phys. Rev. B **86**, 144420 (2012).
[11] S. Seki, X. Z. Yu, S. Ishiwata, and Y. Tokura, Science **336**, 198 (2012).
[12] J. Fukuda and S. Zumer, Nat. Commun. **2**, 246 (2011).
[13] S. Heinze, K. von Bergmann, M. Menzel, J. Brede, A. Kubetzka, R. Wiesendanger, G. Bihlmayer, and S. Blügel, Nat. Phys. **7**, 713 (2011).
[14] A. B. Butenko, A. A. Leonov, U. K. Rößler, and A. N. Bogdanov, Phys. Rev. B **82**, 052403 (2010); E. A. Karhu, U. K. Rößler, A. N. Bogdanov, S. Kahwaji, B. J. Kirby, H. Fritzsche, M. D. Robertson, C. F. Majkrzak, and T. L. Monchesky, *ibid*. **85**, 094429 (2012).
[15] I. E. Dzyaloshinskii, Zh. Eksp. Teor. Fiz. **46**, 1420 (1964) [Sov. Phys. JETP **19**, 960 (1964)]; **47**, 992 (1964) [**20**, 665 (1965)].
[16] P. Bak and M. H. Jensen, J. Phys. C **13**, L881 (1980).
[17] A. Hubert and R. Schäfer, *Magnetic Domains* (Springer, Berlin, 1998).
[18] N. S. Kiselev, A. N. Bogdanov, R. Schäfer, and U. K. Rößler, Phys. Rev. Lett. **107**, 179701 (2011); J. Phys. D **44**, 392001 (2011).
[19] G. H. Wright and N. D. Mermin, Rev. Mod. Phys. **61**, 385 (1989).
[20] U. K. Rößler, A. A. Leonov, and A. N. Bogdanov, J. Phys.: Conf. Ser. **303**, 012105 (2011).
[21] J. Jäykkä and J. Hietarinta, Phys. Rev. D **79**, 125027 (2009).
[22] D. B. Kirk and W. W. Hwu, *Programming Massively Parallel Processors* (Elsevier, Amsterdam, 2010).
[23] A. Vansteenkiste and B. Van de Wiele, J. Magn. Magn. Mater. **323**, 2585 (2011).
[24] See Supplemental Material at http://link.aps.org/supplemental/10.1103/PhysRevB.87.094424 for a demonstration of the magnetic structures of the cone, helicoid, and skyrmion phases in a thin film.